Facilitation of neural responses to targets moving against optic flow

Sarah Nicholas[1] and Karin Nordström[1,2]*

[1]Flinders Health and Medical Research Institute, Flinders University, GPO Box 2100, Adelaide, SA, 5001, Australia

[2]Department of Neuroscience, Uppsala University, Box 593, 751 24 Uppsala, Sweden

*email: karin.nordstrom@flinders.edu.au

ORCIDs

Sarah Nicholas: 0000-0002-5555-9421

Karin Nordström: 0000-0002-6020-6348

Classification

Biological sciences: Neuroscience

Keywords

Target motion, insect vision, motion vision, background motion, hoverfly, TSDN, widefield motion, response suppression, neural facilitation, sensori-motor

Abstract

For the human observer, it can be difficult to follow the motion of small objects, especially when they move against background clutter. In contrast, insects efficiently do this, as evidenced by their ability to capture prey, pursue conspecifics, or defend territories, even in highly textured surrounds. We here recorded from target selective descending neurons (TSDNs) which likely subserve these impressive behaviors. To simulate the type of background optic flow that would be generated by the pursuer's own movements through the world, we used the coherent motion of a perspective distorted sparse dot field. We show that hoverfly TSDN responses to target motion are suppressed when such background optic flow moves in the same direction as the target. Indeed, the neural responses are strongly attenuated against both translational sideslip as well as rotational yaw. More strikingly, we show that TSDNs are facilitated by background optic flow in the opposite direction to the target, if the target moves horizontally. Furthermore, we show that a small, frontal spatial window of background optic flow is enough to fully facilitate or attenuate TSDN responses to target motion. We argue that the TSDN response facilitation could be beneficial in modulating corrective turns during target pursuit.

Significance statement

Target detection in visual clutter is a difficult computational task that insects, with their poor resolution compound eyes and small brains, do successfully and with extremely short behavioral delays. We here show that the responses of target selective descending neurons are attenuated by background motion in the same direction as target motion, but facilitated by opposite direction background motion. This finding is important for understanding conspecific pursuit behavior, since these descending neurons likely control behavioral output. The facilitation that we describe would come into effect if the hoverfly is subjected to background motion in one direction, but the target it is pursuing moves in the opposite direction, and could therefore be used to modulate gaze stabilizing corrective turns.

/body

Introduction

The survival of many animals often depends on their ability to visually detect small moving objects or targets, as these could represent predators, prey, mates or territorial intruders (1). Efficient target detection is a computationally challenging task, which becomes even more difficult when done against visual clutter. Despite this, many insects successfully detect targets, followed by highly acrobatic pursuits, often in visually complex environments. For example, male *Eristalis tenax* hoverflies establish territories in foliage rich areas, on alert for intruders or potential mates and ready to engage in high-speed pursuit (2).

Initial target detection can be facilitated by behaviors that render the background stationary, thus making the target the only thing that moves. Many insects and vertebrates indeed visualize targets against the bright sky (3), or from a stationary stance, such as perching (4-6) or hovering (7, 8). However, as soon as the pursuer moves, its own movement creates self-generated widefield motion across the retina, often referred to as optic flow (9), or background motion (10). In addition to self-generated background optic flow, when a pursuer is subjected to involuntary deviations away from their flight path, for example by a gust of wind, this also generates background optic flow. Quickly correcting such unplanned course deviations is essential for successfully navigating through the world. For example, a flying insect being pushed sideways to the right by a gust of wind, will experience optic flow in the opposite direction. To correct for this, in response to leftward optic flow, the insect will use its wings to perform a corrective optomotor response to the left (11), and/or stabilize its gaze by moving its head (12). Recent evidence, suggests that efference copies suppress the visual neurons sensitive to optic flow, as the optomotor response could otherwise counteract voluntary turns (13).

During pursuit, the pursuer is thus subjected to visual motion that could originate from the independent motion of objects within the environment, from its own intentional movements, or from movement imposed by external forces, such as a gust of wind. Importantly, how the insect moves also affects the type of optic flow it will experience. For

example, during translations distant features move slower than closer ones, whereas during rotations, all features move at the same angular velocity irrespective of distance from the observer (14). Many insects use the information such relative motion provides to estimate the distance to features in the surround. *Eristalis tenax* hoverflies, for example, make both small translational head movements when perched and larger side-to-side movements during flight (15, 16). Moreover, many flying insects, including *Eristalis,* show behavioral segregation between rotational and translational movements, through a saccadic flight and gaze strategy (16-18). How this may influence target detection is currently not known.

The ability of insects to successfully pursue targets in clutter (4, 19) is thus remarkable, and suggests a high level of optimization, making the underlying neural mechanisms interesting to study. Indeed, insects that efficiently pursue targets, including predatory dragonflies and robberflies, as well as territorial hoverflies, have higher-order neurons that are sharply tuned to the motion of small, dark targets, identified in the optic lobes (20, 21) and the descending nerve cord (22, 23). Target tuned neurons often have receptive fields (24-26) in the part of the compound eye that has the best optics (27, 28). Target selective descending neurons (TSDNs) project to the thoracic ganglia (25, 29) where wing and head movements are controlled (30), and electrically stimulating dragonfly TSDNs leads to wing movements (31). Taken together, this suggests that TSDNs subserve target pursuit. However, how TSDNs respond to targets moving against translational and rotational optic flow is unknown.

We quantified the responses of *Eristalis* TSDNs to targets moving against 6 types of optic flow, three translations and three rotations. The background optic flow consisted of the coherent motion of thousands of “targets”, so that the target could only be distinguished by its relative motion. We found that optic flow in the same direction as the target attenuated the TSDN response to the target, whether the optic flow moved in a rotational or translational manner. We found that perpendicular optic flow attenuated the TSDN target response, but to a lesser degree than syn-directional background motion. This suggests that the vector divergence between the target and the background is important. Most strikingly, we found that optic flow in the opposite direction to target motion increased the TSDN response, if the target moved horizontally. Such neural facilitation is a novel observation. We found that a small spatial extent of frontal motion was sufficient to elicit both TSDN

106 attenuation and facilitation, whether spatially overlapping with target motion or not. As
107 descending neurons control behavioral output (30, 31), the response attenuation and
108 facilitation could play a role in modulating optomotor or gaze stabilizing corrective turns as
109 needed during target pursuit.

110 Results

111 *TSDNs respond to target motion but not to background optic flow*

112 We simulated background optic flow using the coherent motion of a sparse dot field (24). By
113 projecting the individual features in the sparse dot field onto a screen anterior of the
114 hoverfly, their spatial location, and simulated z-depth, over time, provided the type of optic
115 flow that would be generated by self-motion (24). In optic flow sensitive descending
116 neurons, this stimulus elicits strong direction-selective responses, similar to the responses
117 to widefield sinusoidal gratings (24), or large moving images (22) with naturalistic statistics
118 (32). We confirmed that our optic flow stimulus did not generate a response in target
119 selective descending neurons (TSDNs) in male *Eristalis tenax* hoverflies (Fig. S1). For
120 example, translational sideslip to the left only generated a response in 18% of 222
121 repetitions across 12 TSDNs (Fig. S1A). Furthermore, when leftward sideslip did generate a
122 TSDN response, this was much less than the response to a target traversing a white
123 background (Fig. S1B). This lack of TSDN response confirms that the optic flow stimulus is
124 qualitatively similar to other types of widefield background motion.

125 In contrast to the lack of response to the optic flow, TSDNs responded strongly to the
126 motion of a small, dark target (22, 24) traversing a white background (compare spiking
127 response during stimulation with the lack of activity before stimulation, Fig. 1, left, Movie 1,
128 2), as well as when the target traversed the stationary sparse dot field (Fig. 1, right, Movie 3,
129 4). Note, that since the sparse dot field consisted of hundreds of “targets”, there were no
130 spatial characteristics separating the individual target from the optic flow when both were
131 stationary (Fig. 1A, right). For quantification across neurons, we calculated the mean spike
132 frequency for the duration of target motion, except for the first and last 40 ms of each 500
133 ms target trajectory (dotted box, Fig. 1B, C). We found a small, but significant response
134 reduction to targets moving across a stationary dot field compared with a white background

135 (Fig. 1D). As the response across neurons was variable (N=30, coefficient of variation 63%
136 and 67%, respectively, Fig. 1D), we normalized the response from each neuron to its own
137 mean response to a target moving across a white background.

138 ***Background optic flow modulates the TSDN target response***

139 To investigate the effect the background optic flow had on TSDN responses to target motion
140 we simulated different types of translations (Fig. 2A) at 50 cm/s and rotations (Fig. 2B) at 50
141 deg/s. During translations distant features move slower than closer ones, whereas during
142 rotations, all features move at the same angular velocity irrespective of distance from the
143 observer (14). We first simulated translational sideslip and found that when the target
144 moved horizontally across syn-directional sideslip, the TSDN response was strongly
145 attenuated (Fig. 2C, D, "Left Sideslip", Movie 5, 6), compared with control where the target
146 moved over a stationary dot field (grey, Fig. 2C, D, Movie 3, 4). Similar effects of syn-
147 directional background motion were previously seen when using panoramic images with
148 naturalistic statistics (22).

149 To investigate the effect the relative motion of individual features within the optic flow had
150 on TSDN responses to target motion, we next simulated rotational yaw at 50 deg/s. We
151 found that yaw optic flow in the same direction as the target also strongly attenuated the
152 TSDN response (Fig. 2C, D, "Left Yaw"). This suggests that rotational and translational optic
153 flow have the same effect on TSDN responses to target motion, and that the relative motion
154 of features within the optic flow is less important.

155 We next investigated the effect opposite-direction background optic flow had on TSDN
156 responses to target motion. We found that when the target moved against counter-
157 directional sideslip the TSDN response was strongly enhanced (Movie 7, 8, Fig. 2C, D, "Right
158 Sideslip", mean increase 71.1%). Similarly, yaw optic flow in the opposite direction to the
159 target also facilitated the TSDN response, by 84.9% (Fig. 2C, D, "Right Yaw"). Such response
160 facilitation was not seen when displaying targets over counter-directional background
161 motion using panoramic images, in either TSDNs (22) or other target tuned neurons in the
162 fly optic lobes (21, 26, 33).

163 ***Frontal optic flow is required and sufficient***

164 Our data show that yaw and sideslip have similar effects on TSDN responses to target
165 motion (Fig. 2). As both sideslip and yaw contain substantial local motion in the frontal
166 visual field (34), we next asked if frontal optic flow is required. We investigated this by
167 limiting the spatial extent of the sideslip to either cover the ipsilateral, dorsal, ventral or
168 contralateral position on the screen (Fig. 3A). Note that only the dorsal position covers the
169 TSDN receptive field (Fig. 3A). In the other three positions, the sideslip optic flow was
170 spatially separated from the receptive field (Fig. 3A), and thus the target trajectory.

171 We found that when sideslip moved in the same direction as the target, the TSDN response
172 was attenuated if the optic flow covered the full, dorsal or ventral position on the screen
173 (Fig. 3B), compared with the stationary control (grey, Fig. 3B). However, when the optic flow
174 only covered the ipsilateral or contralateral positions, there was no difference compared
175 with control (Fig. 3B), suggesting that frontal optic flow is both required and sufficient. Our
176 results are consistent with previous work using moving images with naturalistic statistics,
177 which did not have to spatially overlap with the target trajectory, nor have a large spatial
178 extent, to attenuate TSDN responses (22).

179 We next found that when sideslip moved in the opposite direction to the target, the TSDN
180 response to target motion was facilitated if the optic flow covered the full, dorsal or ventral
181 positions of the screen (Fig. 3C). When the sideslip was limited to the ipsilateral or
182 contralateral positions, there was no TSDN response facilitation (Fig. 3C). This suggests that
183 the optic flow does not have to spatially overlap with the target trajectory. However, there
184 has to be frontal, opposite direction optic flow for facilitation to take place.

185 In summary, our results show that a small spatial window of optic flow in either the dorsal
186 or ventral visual field is enough to strongly attenuate (Fig. 3B) or facilitate (Fig. 3C) the TSDN
187 response to target motion.

188 ***Vector divergence between target and background optic flow affects TSDNs response***

189 Our data above show that syn-directional optic flow strongly attenuates TSDN responses to
190 target motion, whereas counter-directional optic flow facilitates the response (Fig. 2, 3).

191 This suggests that the level of vector divergence between the target and the background
192 influences the TSDN responses, so that maximum attenuation is generated at minimum
193 vector divergence, whereas maximum facilitation is generated at maximum divergence. To
194 explore this in further detail, we quantified the effect other types of optic flow had on TSDN
195 responses to target motion.

196 We found that the TSDN target response was suppressed by lift, which moves perpendicular
197 to the target (mean 44.0% response for downwards lift, “Lift Down”; mean 34.3% for
198 upwards lift, “Lift Up”, Fig. 4). When the target was displayed against pitch, which also
199 provides perpendicular motion in the frontal visual field, the response was suppressed to
200 similar levels (57.1%, “Pitch Down”; 54.9%, “Pitch Up”, Fig. 4). The TSDN response to target
201 motion was also attenuated when the target was displayed against thrust, which provides
202 perpendicular motion along the animal’s anterio-posterior axis (44.3%, “Thrust Towards”;
203 58.4%, “Thrust Away”, Fig. 4). Thus, perpendicular background optic flow attenuates the
204 TSDN response (Fig. 4), but not as much as syn-directional motion (Fig. 2).

205 We next looked at roll optic flow, which creates no local motion straight ahead of the fly,
206 but opposite direction local motion in the dorsal and ventral visual fields. For example,
207 during counter-clockwise roll (“Roll CCW”, Fig. 4) the target and the background optic flow
208 move in the same direction through the dorsal receptive field, but in opposite directions in
209 the ventral visual field. Therefore, the TSDN would receive a combination of maximum and
210 minimum vector divergence signals from the “dorsal” and “ventral” parts (as shown in Fig.
211 3). We found that the response attenuation was stronger against counter-clockwise roll
212 (75.3%, “Roll CCW”, Fig. 4), than against clockwise roll (31.9%, “Roll CW”, Fig. 4).

213 Thus, our data (Fig. 2, 4) support the notion that the level of vector divergence influences
214 the TSDN response. To explore this in further detail, we recorded from TSDNs that respond
215 robustly both to horizontal (grey, Fig. 5) and vertical target motion (black, Fig. 5). We found
216 that when the target moved horizontally, the TSDN response was strongly attenuated
217 against syn-directional sideslip (2nd column, Fig. 5C), less attenuated against lift in either
218 direction (last two columns, Fig. 5C), and strongly facilitated when displayed against
219 counter-directional sideslip (3rd column, Fig. 5C), consistent with previous results (Fig. 2, 4).
220 In the same TSDN neurons, we next moved the target vertically. We found that the TSDN

221 response was completely attenuated against syn-directional lift (last column, Fig. 5D), and
222 less attenuated against sideslip in either direction (2nd and 3rd column, Fig. 5D), which moves
223 perpendicular to the target. This supports the suggestion that maximum TSDN response
224 attenuation is generated at minimum vector divergence between the target and
225 background. However, when the vertical target was displayed against counter-directional
226 lift (4th column, Fig. 5D), there was no response facilitation. This suggests that maximum
227 vector divergence on its own is not enough to explain the TSDN response facilitation to
228 target motion.

229 ***Responses to ON-OFF edges consistent with 1-point correlation***

230 TSDNs have been proposed to get their input from STMDs (35). As opposed to our TSDN
231 data, hoverfly STMD responses are rarely suppressed by syn-directional background motion,
232 and not facilitated by counter-directional background motion (21). As there are many other
233 target tuned neurons in the fly optic lobes (e.g. 33, 36-39) it is possible that TSDNs do not
234 get their input from STMDs. We can investigate the potential input using the underlying
235 target tuning mechanisms, which can be distilled down into three fundamentally different
236 concepts. For example, visual neurons can become target tuned by receiving inhibitory
237 feedback from the widefield system (39-41), or by using center-surround antagonism
238 together with rapid adaptation (38, 42). Alternatively, they can use an elementary STMD
239 model, which is tuned to the unique spatio-temporal profile of a moving target, with a dark
240 contrast change (OFF) from the leading edge followed by a bright contrast change (ON) by
241 the trailing edge. Importantly, while the first two mechanisms rely on comparisons from
242 neighboring points in space, the elementary STMD compares input from one point on space
243 (38, 43, 44). Therefore, the first two models will respond similarly to the motion of a target,
244 to the motion of a leading OFF edge, and the motion of a trailing ON edge (black, Fig. 6,
245 redrawn from (38, 45)). In contrast, the elementary STMD model only responds strongly to
246 the target (grey, Fig. 6, redrawn from (45)).

247 Our results show that TSDNs do not respond well to a leading OFF edge, or to a trailing ON
248 edge (white, Fig. 6). However, a complete target, where the leading edge is rapidly followed
249 by a trailing edge, gives a robust TSDN response (white, Fig. 6). Indeed, the physiological
250 responses (white, Fig. 6) match the elementary STMD model output (grey, Fig. 6). Since

STMD physiology also matches the elementary STMD model output (45, 46), this suggests that TSDNs receive input from STMDs.

Discussion

We found that optic flow moving in the same direction as a target almost completely attenuated the TSDN target response (Fig. 2), even when the optic flow only covered a small part of the frontal visual field (Fig. 3). More strikingly, we found that optic flow in the opposite direction to target motion increased the TSDN response (Fig. 2), if the target moved horizontally (Fig. 5). We also found that perpendicular optic flow attenuated the TSDN target response (Fig. 3, 4), but less than syn-directional motion, suggesting that the vector divergence between the target and the background is important for response suppression. However, we found that vector divergence is not enough to explain the response facilitation (Fig. 3C).

We show for the first time, that TSDN responses to target motion are facilitated by counter-directional optic flow (Fig. 2). Such neural facilitation has not been seen in previous work in TSDNs (22) or STMDs (21, 26, 46), or other target tuned neurons in the optic lobes (33, 36, 39). Instead, in our previous work TSDN responses were significantly reduced when a background image with naturalistic statistics moved in the opposite direction to the target (22). Since the background used previously drive optic flow sensitive descending neurons as well as sinusoidal gratings do (22, 47), and as well as the sparse dot field used here (24), this suggests that facilitation is not generated by widefield motion in general. Indeed, this suggests that there is something fundamentally different about the optic flow used here, and the backgrounds in previous work. One difference is that we here use perspective distorted optic flow, where the individual features move faster the closer they are during translations, whereas during rotations they all move at the same angular velocity irrespective of distance from the viewer. However, we found that the facilitation was strong whether the target was displayed over sideslip or yaw (Fig. 2), suggesting that the relative motion of the features within the background optic flow is not important.

Another difference is that the background used here consisted of the coherent motion of thousands of “targets”, whereas previous TSDN work used a background image with

280 naturalistic statistics (22). We currently do not know how STMDs, which are likely pre-
281 synaptic to the TSDNs (Fig. 6, and see Ref. 35), respond to this stimulus. However, we do
282 know that STMDs generate their ability to detect targets in clutter by being sharply tuned to
283 the target's unique spatio-temporal profile (43), with a dark-contrast OFF edge quickly
284 followed by a bright-contrast ON edge (Fig. 6). Indeed, if naturalistic backgrounds contain
285 small, high-contrast features, these often generate STMD responses (46). However, despite
286 our optic flow consisting of "targets", we saw no consistent TSDN responses even to
287 preferred direction motion (e.g. "Sideslip Left", "Yaw Left", Fig. S1, Movie 5, 6). This
288 suggests that TSDNs do not filter contrasting targets embedded within a background, like
289 some STMDs do (21, 46).

290 It is thus difficult to determine whether the facilitation is driven by active facilitation onto
291 the TSDN, or if it is inherited from upstream processes. If it is generated by neural input, and
292 since the facilitation required frontal optic flow, but this did not have to spatially overlap
293 with the TSDN receptive field or the target trajectory (Fig. 3A, C), the facilitation would
294 come from a direction-selective neuron type with a frontal visual field. Since counter-
295 directional lift did not facilitate the TSDN response if the target moved vertically rather than
296 horizontally (Fig. 5C), this suggests that such a neuron would have to be most sensitive to
297 horizontal motion, and less to vertical motion. Since some STMDs might respond to features
298 within the optic flow used here (46), and furthermore, since there are some STMDs that
299 respond both to target motion and to features within background motion (21), these could
300 potentially play a role in this. Future investigation of STMD and TSDN responses are clearly
301 required to explore the underlying mechanisms.

302 In contrast to the facilitation, we found that the sparse dot field stimulus suppressed the
303 TSDN response to target motion when these moved in the same direction (Fig. 2). This
304 response suppression could be driven by active inhibition from widefield motion detectors,
305 as previously suggested (22), or inherited from upstream processes. We previously showed
306 that TSDN responses to target motion are suppressed by background motion consisting of
307 an image with naturalistic statistics, and that background stimuli that drive optic flow
308 sensitive neurons suppress TSDN responses to target motion, whether spatially overlapping
309 with the target trajectory or not (22). This suggests that TSDNs are suppressed by widefield

310 motion in general. However, note that since we found maximum TSDN response
311 suppression at minimum vector divergence, whereas perpendicular motion suppressed the
312 response less (Fig. 4, 5; and see ref. 22), the response suppression has to contain some type
313 of vector divergence comparison.

314 Nevertheless, our findings make behavioral sense. Prior to initiating target pursuit, male
315 *Eristalis* hoverflies predict the flight course required to successfully intercept the target,
316 based predominantly on the target's angular velocity (48). To successfully execute an
317 interception style flight course, the hoverfly turns in the direction that the target is moving
318 (48). In doing so, the hoverfly creates self-generated optic flow in the opposite direction to
319 the target's motion. In this case the TSDNs would be facilitated (Fig. 2), which could be
320 beneficial.

321 Once pursuit is initiated, if the pursuer drifts rightward due to e.g. a gust of wind, this
322 induces leftward optic flow across the frontal retina, which would evoke a leftward
323 optomotor response and/or gaze stabilizing turn. If the target is also moving leftward, in the
324 direction of the corrective maneuver, this maneuver would also pursue the target and no
325 TSDN signal would be required. Indeed, we found that the TSDNs were quiet under such
326 conditions ("Left", Fig. 2). However, if during the same pursuit the target instead moves
327 rightward, opposite to the direction of the pursuer's corrective maneuver, then the TSDNs
328 would be strongly facilitated ("Right", Fig. 2). Considering that TSDNs project to motor
329 command centers in the thoracic ganglia (25, 31), this TSDN facilitation could then
330 presumably override corrective turns. The TSDN response modulation by optic flow shown
331 here could thus be beneficial for controlling behavioral output.

332 We only saw a response facilitation if the target moved horizontally, and not vertically (Fig.
333 5). This facilitation difference could be affected by the fact that the TSDNs that we recorded
334 from responded better to horizontal motion than to vertical target motion (Fig. 5A). In
335 addition, since we do not know where the TSDNs project to we do not know if the TSDNs
336 control head movements, wing movements, or maybe both. Indeed, recent work suggests
337 that gaze stabilizing turns by the head, and the wing optomotor response, are controlled
338 independently, and by different visual components (12, 49, 50). Furthermore, the difference
339 could be explained by different behavioral requirements to vertical and horizontal target

340 deviations. For example, whereas horizontal deviations require the left and right wings to
341 move differently, to induce a turn, vertical deviations would likely require the left and right
342 wings to perform similar corrective behaviors. Finally, it is important to note that even if the
343 responses to vertical target motion were not facilitated, neither were they suppressed (4th
344 column, Fig. 5D). There would thus still be a strong neural signal projected to the thoracic
345 ganglia.

346 Materials and Methods

347 *Electrophysiology*

348 *Eristalis tenax* hoverflies were reared and maintained as previously described (51). For
349 electrophysiology, a male hoverfly was immobilized ventral side up using a beeswax and
350 resin mixture. A small hole was cut at the anterior end of the thorax to expose the cervical
351 connective, which was then raised slightly and supported using a small wire hook, for
352 insertion of a sharp polyimide-insulated tungsten microelectrode (2 MOhm, Microprobes,
353 Gaithersburg, USA). The animal was grounded via a silver wire inserted into the ventral part
354 of the hole.

355 Extracellular signals were amplified at 100x gain and filtered through a 10- to 3000-Hz
356 bandwidth filter on a DAM50 differential amplifier (World Precision Instruments, Sarasota,
357 USA), with 50 Hz noise removed with a HumBug (Quest Scientific, North Vancouver,
358 Canada). The data were digitized via Powerlab 4/30 (ADInstruments, Sydney, Australia) and
359 acquired at 40 kHz with LabChart 7 Pro software (ADInstruments). Single units were
360 discriminated by amplitude and half-width using Spike Histogram software (ADInstruments).

361 *Visual stimuli*

362 *Eristalis* males were placed ventral side up, centered and perpendicular to an Asus LCD
363 screen (Asus, Taipai, Taiwan) at 6.5 cm distance. The screen had a refresh rate of 165 Hz, a
364 linearized contrast with a mean illuminance of 200 Lux, and a spatial resolution of 2560 x
365 1440 pixels, giving a projected screen size of 155° x 138°. Visual stimuli were displayed using
366 custom written software based on the Psychophysics toolbox (52, 53) in Matlab
367 (Mathworks, Natick, USA).

368 TSDNs were identified as described (22, 24). In short, we mapped the receptive field of each
369 neuron by scanning a target horizontally and vertically at 20 evenly spaced elevations and
370 azimuths (24), to calculate the local motion sensitivity and local preferred direction. We
371 then scanned targets of varying height through the small, dorso-frontal receptive fields (Fig.
372 3A) to confirm that each neuron was sharply size tuned with a peak response to targets
373 subtending 3°- 6°, with no response to larger bars, to looming or to widefield stimuli (22,
374 24).

375 Unless otherwise mentioned, targets were black and round with a diameter of 15 pixels,
376 moving at a velocity of 900 pixels/s for 0.48 s. When converted to angular values and taking
377 the small frontal receptive fields of TSDNs into account, this corresponds to an average
378 diameter of 3° and a velocity of 130°/s (22). Unless otherwise stated, each target travelled in
379 each neuron's preferred horizontal direction (i.e. left or right) and across the center of its
380 receptive field. Between repetitions, we varied the target elevation slightly, to minimize
381 habituation (22). There was a minimum 4 s between stimulus presentations. Stimulus order
382 was randomized.

383 Optic flow was generated as previously described (24). Briefly, the optic flow consisted of a
384 simulated cube with 4 m sides, filled with 2 cm diameter spheres at a density of 100 per m^3,
385 with the hoverfly placed in the center. The coherent motion of these ca 6400 spheres
386 around the hoverfly was used to simulate self-generated optic flow. The ca 1200 spheres
387 anterior to the hoverfly were projected onto the screen, with their size indicating the
388 distance from the hoverfly. Circles closer than 6 cm were not displayed. Six types of optic
389 flow were simulated: three translations at 50 cm/s (sideslip, lift and thrust) and three
390 rotations at 50°/s (yaw, pitch and roll). Unless otherwise stated optic flow was displayed for
391 0.48 s prior to the target. Both target motion and optic flow disappeared simultaneously.

392 In most experiments the optic flow covered the entire visual display. In some experiments,
393 we limited the spatial extent of the optic flow, into 4 spatial positions (Fig. 3A). TSDN
394 receptive fields tend to be located slightly offset from the visual midline, with preferred
395 direction of motion away from the midline (Fig. 3A). We defined the lateral parts of the
396 display as either ipsilateral or contralateral based on the preferred direction of each TSDN.

397 ***Data analysis and statistics***

398 We recorded from 30 TSDNs in 30 male hoverflies. We kept data from all TSDNs that
399 showed a robust response to a target moving over a white background (Fig. 1, Movie 1, 2).
400 We repeated this control throughout the recording, and only kept data from neurons that
401 responded consistently. We only kept data from experiments with a minimum 9 repetitions.
402 The data from repetitions within a neuron were averaged, and shown as spike histograms
403 (mean ± sem) with 1 ms resolution, after smoothing with a 20 ms square-wave filter. For
404 quantification across neurons, we calculated the mean spike rate for each neuron from the
405 spike histogram for the duration of target motion, after excluding the first and last 40 ms of
406 each 0.48 s target trajectory (dotted boxes, Fig. 1B, C), unless otherwise indicated. We
407 normalized the responses to each neuron's own mean response to a target moving over a
408 white background.

409 Data analysis was performed in Matlab and statistical analysis in Prism 7.0c for Mac OS X
410 (GraphPad Software, San Diego, USA). Throughout the paper *n* refers to the number of
411 repetitions within one neuron, and *N* to the number of neurons. The sample size, type of
412 test (paired t-tests or one-way ANOVAs, followed by Dunnett's post hoc test for multiple
413 comparisons) and P value is indicated in each figure legend. All data have been deposited to
414 DataDryad.

415 **Acknowledgements**

416 We thank current and past lab members for constructive feedback, and the Botanic Gardens
417 of Adelaide for their ongoing support. Malin Thyselius provided the hoverfly pictogram in
418 Fig. 2. Our research was funded by the US Air Force Office of Scientific Research (AFOSR,
419 FA9550-19-1-0294), the Australian Research Council (ARC, DP170100008, DP180100144 and
420 FT180100289), and the Flinders Foundation.

421

References

1. P. T. Gonzalez-Bellido, S. T. Fabian, K. Nordström, Target detection in insects: optical, neural and behavioral optimizations. *Curr Opin Neurobiol* **41**, 122-128 (2016).
2. W. Wellington, S. Fitzpatrick, Territoriality in the drone fly, *Eristalis tenax* (Diptera, Syrphidae). *Can Entomol* **113**, 695-704 (1981).
3. J. Zeil, Sexual dimorphism in the visual system of flies: The free flight behavior of male Bibionidae (Diptera). *J Comp Physiol A* **150**, 395-412 (1983).
4. S. T. Fabian, M. E. Sumner, T. J. Wardill, S. Rossoni, P. T. Gonzalez-Bellido, Interception by two predatory fly species is explained by a proportional navigation feedback controller. *Journal of The Royal Society Interface* **15** (2018).
5. R. Schröder, C. N. Linkem, J. A. Rivera, M. A. Butler, Should I stay or should I go? Perching damselfly use simple colour and size cues to trigger flight. *Animal Behaviour* **145**, 29-37 (2018).
6. C. T. O'Rourke, T. Pitlik, M. Hoover, E. Fernández-Juricic, Hawk eyes II: diurnal raptors differ in head movement strategies when scanning from perches. *PLoS One* **5**, e12169 (2010).
7. S. M. Fitzpatrick, W. G. Wellington, Contrasts in the territorial behavior of three species of hover flies (Diptera: Syrphidae). *Can Entomol* **115**, 559-566 (1983).
8. E. L. Corvidae, R. O. Bierregaard, S. E. Peters, Comparison of wing morphology in three birds of prey: correlations with differences in flight behavior. *J Morphol* **267**, 612-622 (2006).
9. J. J. Koenderink, Optic flow. *Vision Res* **26**, 161-179 (1986).

10. W. Reichardt, M. Egelhaaf, A. Guo, Processing of figure and background motion in the visual system of the fly. *Biol Cybern* **61**, 327-345 (1989).

11. W. Reichardt, T. Poggio, Visual control of orientation behaviour in the fly. Part I. A quantitative analysis. *Q Rev Biophys* **9**, 311-375 (1976).

12. J. L. Fox, M. A. Frye, Figure-ground discrimination behavior in *Drosophila*. II. Visual influences on head movement behavior. *J Exp Biol* **217**, 570-579 (2014).

13. A. J. Kim, J. K. Fitzgerald, G. Maimon, Cellular evidence for efference copy in *Drosophila* visuomotor processing. *Nat Neurosci* **18**, 1247-1255 (2015).

14. M. Egelhaaf, R. Kern, J. P. Lindemann, Motion as a source of environmental information: a fresh view on biological motion computation by insect brains. *Front Neural Circuits* **8** (2014).

15. W. G. Wellington, S. M. Fitzpatrick, Territoriality in the Drone Fly, Eristalis-Tenax (Diptera, Syrphidae). *Can Entomol* **113**, 695-704 (1981).

16. B. R. Geurten, R. Kern, E. Braun, M. Egelhaaf, A syntax of hoverfly flight prototypes. *J Exp Biol* **213**, 2461-2475 (2010).

17. C. Schilstra, J. H. Hateren, Blowfly flight and optic flow. I. Thorax kinematics and flight dynamics. *The Journal of Experimental Biology* **202**, 1481 (1999).

18. N. Boeddeker, L. Dittmar, W. Stürzl, M. Egelhaaf, The fine structure of honeybee head and body yaw movements in a homing task. *Proceedings of the Royal Society B: Biological Sciences* **277**, 1899-1906 (2010).

19. T. S. Collett, Angular tracking and the optomotor response. An analysis of visual reflex interaction in a hoverfly. *J Comp Physiol A* **140**, 145-158 (1980).

20. D. O'Carroll, Feature-detecting neurons in dragonflies. *Nature* **362**, 541-543 (1993).

467 21. K. Nordström, P. D. Barnett, D. C. O'Carroll, Insect detection of small targets moving
468 in visual clutter. *PLoS Biol* **4**, 378-386 (2006).
469 22. S. Nicholas, J. Supple, R. Leibbrandt, P. T. Gonzalez-Bellido, K. Nordström, Integration
470 of small- and wide-field visual features in Target-Selective Descending Neurons of
471 both predatory and non-predatory dipterans. *J Neurosci* **38**, 10725-10733 (2018).
472 23. M. A. Frye, R. M. Olberg, Visual receptive field properties of feature detecting
473 neurons in the dragonfly. *J Comp Physiol A* **177**, 569-576 (1995).
474 24. S. Nicholas, R. Leibbrandt, K. Nordström, Visual motion sensitivity in descending
475 neurons in the hoverfly. *J Comp Physiol A* **206**, 149-163 (2020).
476 25. P. T. Gonzalez-Bellido, H. Peng, J. Yang, A. P. Georgopoulos, R. M. Olberg, Eight pairs
477 of descending neurons in the dragonfly give wing motor centers accurate population
478 vector of prey direction. *Proc Natl Acad Sci USA* **110**, 676-701 (2013).
479 26. P. D. Barnett, K. Nordström, D. C. O'Carroll, Retinotopic organization of small-field-
480 target-detecting neurons in the insect visual system. *Curr Biol* **17**, 569-578 (2007).
481 27. A. D. Straw, E. J. Warrant, D. C. O'Carroll, A 'bright zone' in male hoverfly (*Eristalis*
482 *tenax*) eyes and associated faster motion detection and increased contrast
483 sensitivity. *J Exp Biol* **209**, 4339-4354 (2006).
484 28. G. A. Horridge, The separation of visual axes in apposition compound eyes. *Philos*
485 *Trans R Soc Lond B Biol Sci* **285**, 1-59 (1978).
486 29. R. M. Olberg, Identified target-selective visual interneurons descending from the
487 dragonfly brain. *J Comp Physiol A* **159**, 827-840 (1986).
488 30. C. T. Hsu, V. Bhandawat, Organization of descending neurons in *Drosophila*
489 *melanogaster*. *Sci Rep* **6**, 20259 (2016).

31. R. M. Olberg (1978) Visual and multimodal interneurons in dragonflies. (University of Washington, Seattle).

32. O. Dyakova, M. Mueller, M. Egelhaaf, K. Nordström, Image statistics of the environment surrounding freely behaving hoverflies. *J Comp Physiol A* **205**, 373-385 (2019).

33. C. Städele, M. F. Keleş, J. M. Mongeau, M. A. Frye, Non-canonical receptive field properties and neuromodulation of Feature-Detecting neurons in flies. *Curr Biol* 10.1016/j.cub.2020.04.069 (2020).

34. M. O. Franz, H. G. Krapp, Wide-field, motion-sensitive neurons and matched filters for optic flow fields. *Biol Cybern* **83**, 185-197 (2000).

35. K. Nordström, D. C. O'Carroll, Feature detection and the hypercomplex property in insects. *Trends Neurosci* **32**, 383-391 (2009).

36. M. F. Keleş, B. J. Hardcastle, C. Städele, Q. Xiao, M. A. Frye, Inhibitory interactions and columnar inputs to an object motion detector in *Drosophila*. *Cell Rep* **30**, 2115-2124.e2115 (2020).

37. M. F. Keleş, M. A. Frye, Object-detecting neurons in *Drosophila*. *Curr Biol* **27**, 680-687 (2017).

38. R. Tanaka, D. A. Clark, Object-displacement-sensitive visual neurons drive freezing in *Drosophila*. *Curr Biol* 10.1016/j.cub.2020.04.068 (2020).

39. M. Egelhaaf, On the neuronal basis of figure-ground discrimination by relative motion in the visual system of the fly. II. Figure-detection cells, a new class of visual interneurones. *Biol Cybern* **52**, 195-209 (1985).

512 40. A. K. Warzecha, M. Egelhaaf, A. Borst, Neural circuit tuning fly visual interneurons to
513 motion of small objects. I. Dissection of the circuit by pharmacological and
514 photoinactivation techniques. *J Neurophysiol* **69**, 329-339 (1993).
515 41. W. Reichardt, T. Poggio, Figure-ground discrimination by relative movement in the
516 visual-system of the fly. Part I: Experimental results. *Biol Cybern* **35**, 81-100 (1979).
517 42. T. Collett, Visual neurones in the anterior optic tract of the privet hawk moth. *J Comp*
518 *Physiol* **78**, 396-433 (1972).
519 43. S. D. Wiederman, P. A. Shoemaker, D. C. O'Carroll, A model for the detection of
520 moving targets in visual clutter inspired by insect physiology. *PLoS ONE* **3**, e2784
521 (2008).
522 44. M. Egelhaaf, On the neuronal basis of figure-ground discrimination by relative
523 motion in the visual system of the fly. III. Possible input circuitries and behavioral
524 significance of the FD-cells. *Biol Cybern* **52**, 267-280 (1985).
525 45. S. D. Wiederman, P. A. Shoemaker, D. C. O'Carroll, Correlation between OFF and ON
526 Channels Underlies Dark Target Selectivity in an Insect Visual System. *J Neurosci* **33**,
527 13225-13232 (2013).
528 46. S. D. Wiederman, D. C. O'Carroll, Discrimination of features in natural scenes by a
529 dragonfly neuron. *J Neurosci* **31**, 7141-7144 (2011).
530 47. S. Nicholas, K. Nordström, Persistent firing and adaptation in optic flow sensitive
531 descending neurons. *Curr Biol* **30**, 2739-2748.e2732 (2020).
532 48. T. S. Collett, M. F. Land, How hoverflies compute interception courses. *J Comp*
533 *Physiol A* **125**, 191-204 (1978).

49. J. L. Fox, J. W. Aptekar, N. M. Zolotova, P. A. Shoemaker, M. A. Frye, Figure-ground discrimination behavior in *Drosophila*. I. Spatial organization of wing-steering responses. *J Exp Biol* **217**, 558-569 (2014).

50. B. Cellini, J. M. Mongeau, Active vision shapes and coordinates flight motor responses in flies. *Proc Natl Acad Sci U S A* **117**, 23085-23095 (2020).

51. S. Nicholas, M. Thyselius, M. Holden, K. Nordström, Rearing and long-term maintenance of *Eristalis tenax* hoverflies for research studies. *JoVE* doi:10.3791/57711, e57711 (2018).

52. D. H. Brainard, The Psychophysics toolbox. *Spatial Vision* **10**, 433-436 (1997).

53. D. G. Pelli, The VideoToolbox software for visual psychophysics: Transforming numbers into movies. *Spatial Vision* **10**, 437-442 (1997).

547 ## Figure Legends

548 ***Figure 1. TSDN response to target motion***

549 **A)** Pictograms of the round, black target, with a diameter of 3°, traversing a white
550 background (left), or stationary optic flow (right), at 130°/s. **B)** Raw data trace from an
551 extracellular TSDN recording. Timing of stimulus presentation indicated by colored bars
552 (blue, target, and red, sparse dot field). **C)** Magnification of the raw data traces shown in
553 panel B. **D)** The mean spiking response of different TSDNs was significantly reduced when
554 the target moved across a stationary sparse dot field compared with a white background
555 (N=30; ***P = 0.0005, two-tailed paired t-test).

556 ***Figure 2. TSDN response to target motion is affected by horizontal background optic flow***

557 **A)** A pictogram indicating the three different types of translations, as seen by the hoverfly.
558 Sideslip was displayed to the left or the right, lift up or down, and thrust towards or away
559 from the hoverfly, all at 50 cm/s. **B)** The three different types of rotations used. As these
560 were simulated to rotate around the hoverfly's position (24), the optic flow displayed on the
561 screen can be described as yaw to the left or the right, pitch up or down, and clockwise or
562 counter-clockwise roll, all at 50 deg/s. **C)** The TSDN response to a target traversing a
563 stationary sparse dot field (left, grey), sideslip or yaw in either the same or the opposite
564 direction to the target (red pictograms). All histograms from a single TSDN (mean ± sem,
565 n=18) shown with 1 ms resolution after smoothing with a 20 ms square-wave filter. **D)** The
566 mean response across TSDNs (N=12) to a target traversing stationary optic flow (left, grey),
567 sideslip or yaw, in the same direction (Left") or opposite direction ("Right") to the target,
568 after normalizing the data to each neuron's own response to a target traversing a white
569 background. The line shows the mean and the filled data points correspond to the neuron in
570 panel C. In panel D significance is shown with **** for P < 0.0001 following a one-way
571 ANOVA followed by Dunnett's multiple comparison's test done together with the data
572 shown in Fig. 4.

573 ***Figure 3. Frontal optic flow is required and sufficient***

574 **A)** A pictogram of the separation of the background optic flow into four distinct positions:
575 ipsilateral (IL), dorsal (D), ventral (V) and contralateral (CL). The color coding shows the
576 receptive field of an example TSDN, and the arrows its local motion sensitivity. **B)** TSDN
577 responses to targets moving across syn-directional sideslip are significantly inhibited
578 compared to stationary control (grey) if the sideslip covers the full, dorsal or ventral screen.
579 **C)** TSDN responses to targets moving across opposite direction sideslip are significantly
580 facilitated compared to stationary control (grey, same data as in panel B) if the sideslip
581 covers the full, dorsal or ventral visual field. Panels B and C show data from the same
582 neurons (N=10, one-way ANOVA followed by Dunnett's multiple comparisons test, with
583 *P<0.05, **P<0.01).

584 ***Figure 4. The TSDN response to target motion is attenuated by perpendicular optic flow***

585 **A)** The response from one TSDN to a target traversing a stationary sparse dot field (left,
586 grey, replotted from Fig. 2C), or different types of optic flow (red pictograms). All histograms
587 shown as mean ± sem (n=18) at 1 ms resolution, after smoothing with a 20 ms square-wave
588 filter. **B)** The mean response across TSDNs (N=12, same neurons as Fig. 2D) to a target
589 traversing a stationary sparse dot field (left, grey, replotted from Fig. 2D), or different types
590 of optic flow. Stars indicate significance, one-way ANOVA followed by Dunnett's multiple
591 comparisons test (**P<0.01, ***P<0.001 and ****P<0.0001), done together with the data
592 shown in Fig. 2D. Translations were simulated at 50 cm/s and rotations at 50°/s. The lines
593 show the mean and the filled data points correspond to the neuron in panel A.

594 ***Figure 5. Vector divergence between optic flow and target***

595 **A)** The TSDN response to a target traversing a white background horizontally (left, grey) or
596 vertically (right, black). Histograms shown as mean ± sem (n=18) at 1 ms resolution, after
597 smoothing with a 20 ms square-wave filter. **B)** The mean spiking response of 8 TSDNs to
598 targets moving horizontally (grey, left) or vertically (black, right) over a white background.
599 The filled data points correspond to the neuron in panel A. **C)** TSDN responses to targets
600 moving horizontally across sideslip or lift, in the same direction as the target, or
601 perpendicular to the target, as indicated by the pictograms. Significance shown using one-
602 way ANOVA followed by Dunnett's multiple comparisons test, with *P=0.0232, **P=0.006,

603 ***P=0.0003, ****P<0.0001. **D)** TSDN responses to targets moving vertically across sideslip
604 or lift, in the opposite direction to the target, or perpendicular to the target, as indicated by
605 the pictograms. Significance shown using one-way ANOVA followed by Dunnett's multiple
606 comparisons test, with *P=0.0198, **P=0.0021, ****P<0.0001. Same N=8 in panels B-D.

607 ***Figure 6. Elementary STMD input to TSDNs***

608 Responses to a leading OFF edge, trailing ON edge, or a complete black target, with a side of
609 3°, traversing a white background at 130°/s. The black data show the predicted output from
610 a motion detector that compares luminance changes from at least 2 points in space. Data
611 replotted from (45), after normalizing to its own sum. The grey data show the predicted
612 output from an elementary STMD (ESTMD), which compares luminance changes from one
613 point in space. Data replotted from (45), after normalizing to its own sum. The white data
614 show the TSDN response to the same three stimuli (N=6) after normalizing the data from
615 each neuron to its own sum.

616

617 ## Supplementary Information

618 ***Figure S1. TSDNs do not respond to optic flow***

619 **A)** To determine the TSDN response to the optic flow we first quantified each neuron's
620 spontaneous rate, i.e. the spikes generated when viewing a white background, and used this
621 as a threshold. For each neuron we then quantified the number of trials in which the
622 response to the optic flow was above this threshold. This was converted to a percentage of
623 responses. The data here show this percentage of responses across 12 TSDNs as mean ±
624 sem. **B)** In each neuron, we quantified the mean response for those trials that were
625 classified as responders (in panel A). This mean response was normalized to each neuron's
626 mean response to a target traversing a white background, as throughout the rest of the
627 paper. Data are shown as mean ± sem (N=12).

628 ***Movie 1. TSDN response to a target over a white background***

629 The movie depicts the stimulus as displayed on the screen, with the hoverfly positioned
630 centered and perpendicular to the screen. The hoverfly was positioned ventral side up, but
631 we have rotated the movie for display purposes so the dorsal side is up. The colored lines
632 show the outline of the receptive field, mapped as described previously (24). The red data at
633 the bottom of the movie show the response of an example TSDN.

634 ***Movie 2. TSDN response to a target over a white background***

635 Same as Movie 1, but slowed down 10 times.

636 ***Movie 3. TSDN response to a target over stationary optic flow***

637 The movie depicts the stimulus as displayed on the screen, with the colored lines showing
638 the outline of the receptive field. The red data at the bottom of the movie show the
639 response of an example TSDN. In this case the optic flow was stationary, and appeared 0.5 s
640 before the target.

641 ***Movie 4. TSDN response to a target over stationary optic flow***

Same as Movie 3, but slowed down 10 times.

Movie 5. TSDN response to a target over syn-directional sideslip

The movie depicts the response of the same example TSDN to the same target motion as in previous movies, but now traversing sideslip appearing 0.5 s before the target. The hoverfly was positioned at a distance of 6.5 cm. At this viewing distance, the resulting optic flow simulates the type of optic flow that would be generated by the hoverfly side-slipping through the world at 50 cm/s. The simulated optic flow consisted of ca 6400 spheres, of which roughly 1200 are projected onto the screen at any one time.

Movie 6. TSDN response to a target over syn-directional sideslip

Same as Movie 5, but slowed down 10 times. Note that many of the optic flow “targets” of the correct size move through the receptive field (colored contour lines).

Movie 7. TSDN response to a target over opposite direction sideslip

The movie depicts the response of the same example TSDN to the same target motion as in previous movies, but now traversing sideslip in the opposite direction to the target.

Movie 8. TSDN response to a target over opposite direction sideslip

Same as Movie 7, but slowed down 10 times.

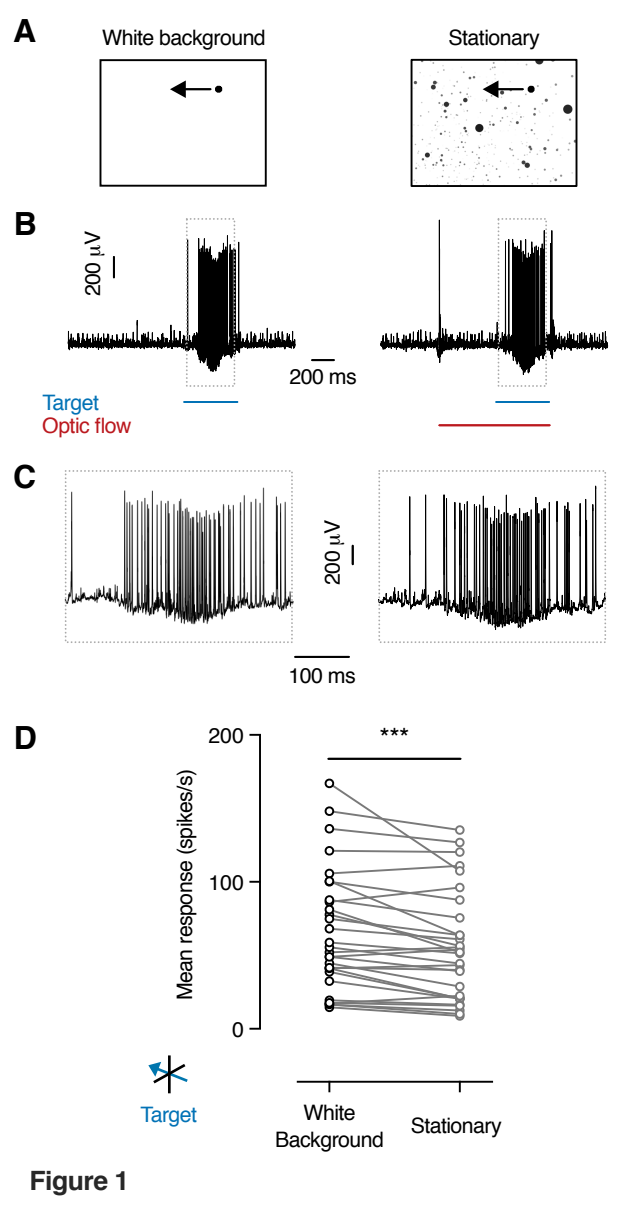
A
White background
Stationary
B
200 µV
200 ms
Target
Optic flow
C
200 µV
100 ms
D
200
100
0
Mean response (spikes/s)
***
Target
White Background
Stationary

Figure 1

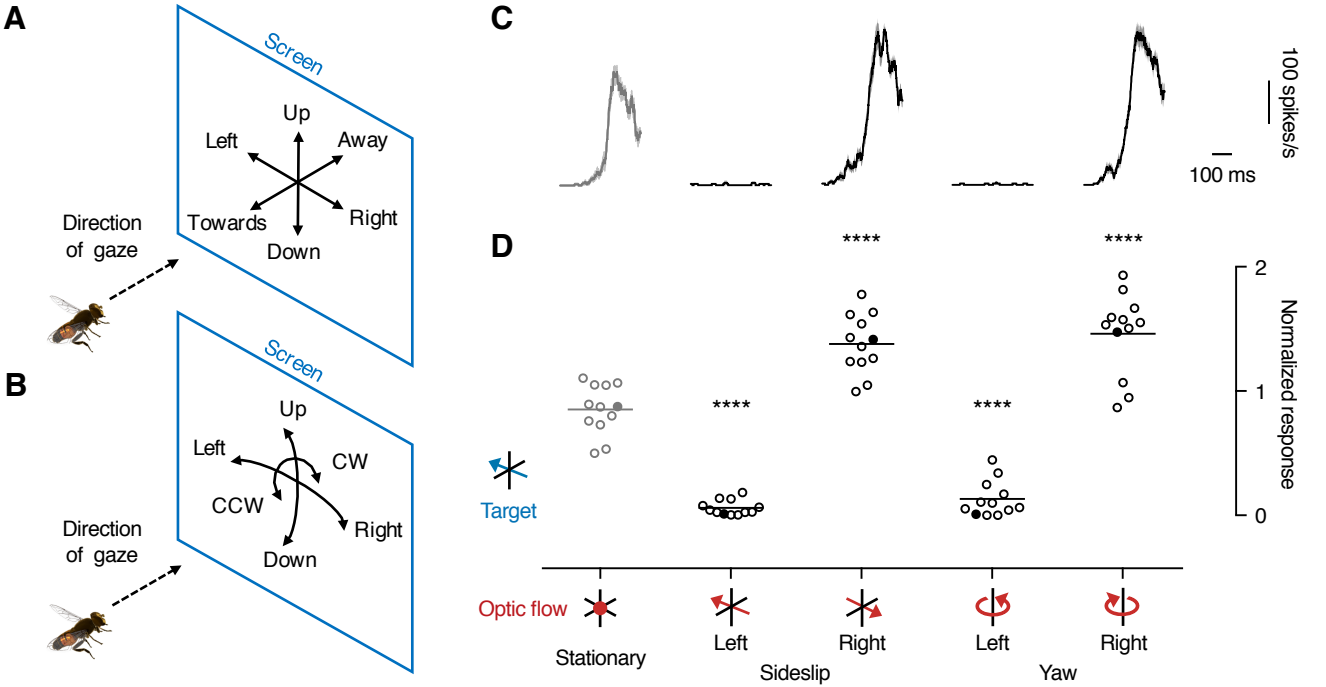
A
Screen
Up
Left
Away
Towards
Right
Down
Direction of gaze
B
Screen
Up
Left
CW
CCW
Right
Down
Direction of gaze
C
100 spikes/s
100 ms
D
****
****
****
****
Normalized response
2
1
0
Target
Optic flow
Stationary
Left
Right
Left
Right
Sideslip
Yaw

Figure 2

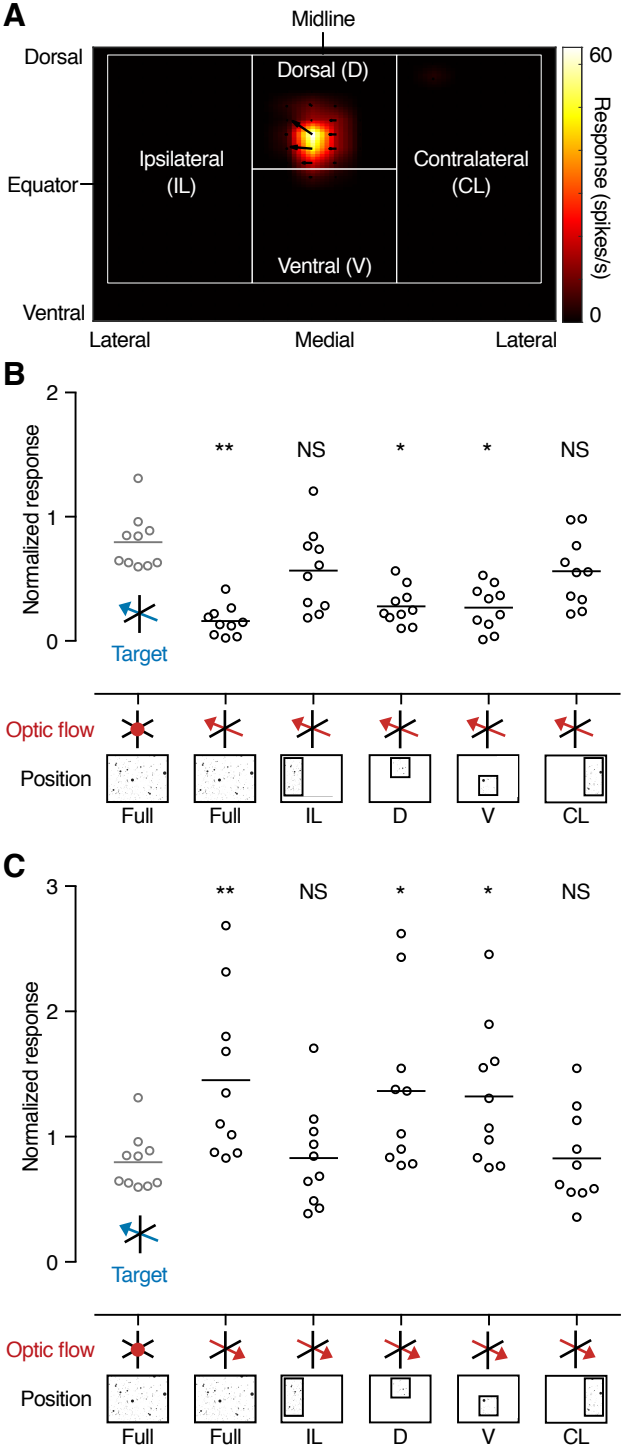
A
Midline
Dorsal
Equator
Ventral
Dorsal (D)
Ipsilateral (IL)
Contralateral (CL)
Ventral (V)
60
Response (spikes/s)
0
Lateral
Medial
Lateral
B
Normalized response
2
1
0
**
NS
*
*
NS
Target
Optic flow
Position
Full
Full
IL
D
V
CL
C
Normalized response
3
2
1
0
**
NS
*
*
NS
Target
Optic flow
Position
Full
Full
IL
D
V
CL

Figure 3

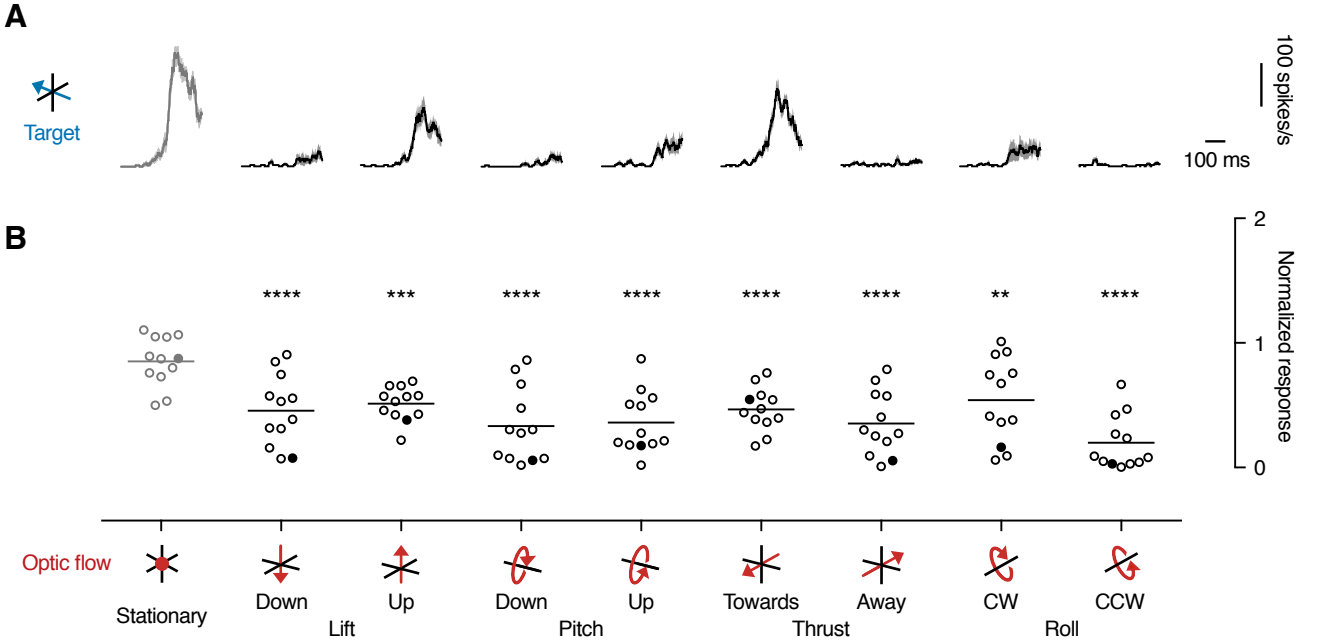
A
Target
100 spikes/s
100 ms
B
Normalized response
2
1
0
****
***
****
****
****
****
**
****
Optic flow
Stationary
Down
Up
Down
Up
Towards
Away
CW
CCW
Lift
Pitch
Thrust
Roll

Figure 4

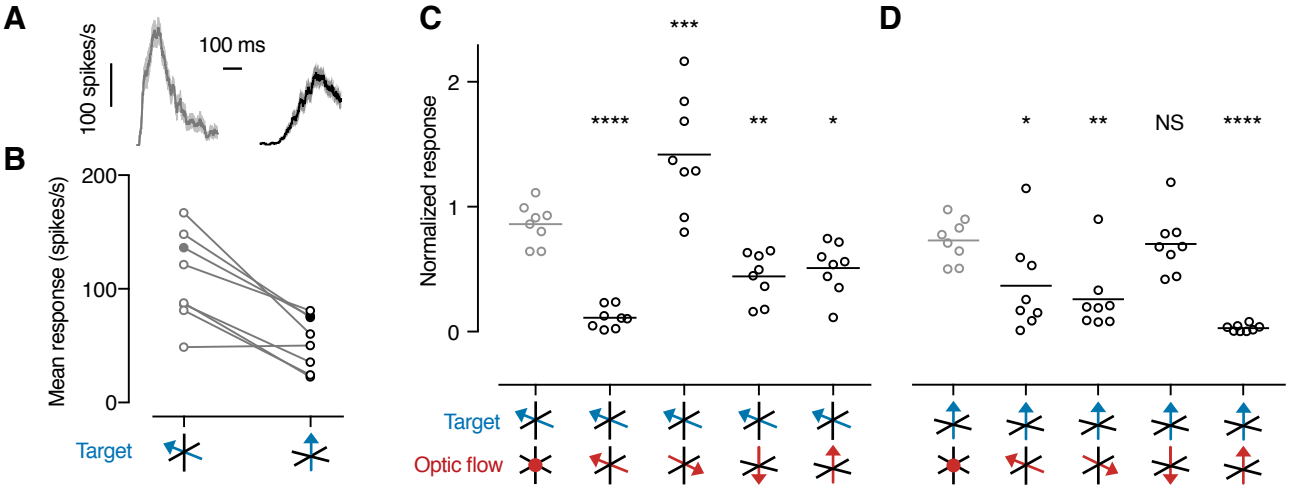
A
100 spikes/s
100 ms
B
Mean response (spikes/s)
200
100
0
Target
C
Normalized response
2
1
0
****
***
**
*
Target
Optic flow
D
*
**
NS
****

Figure 5

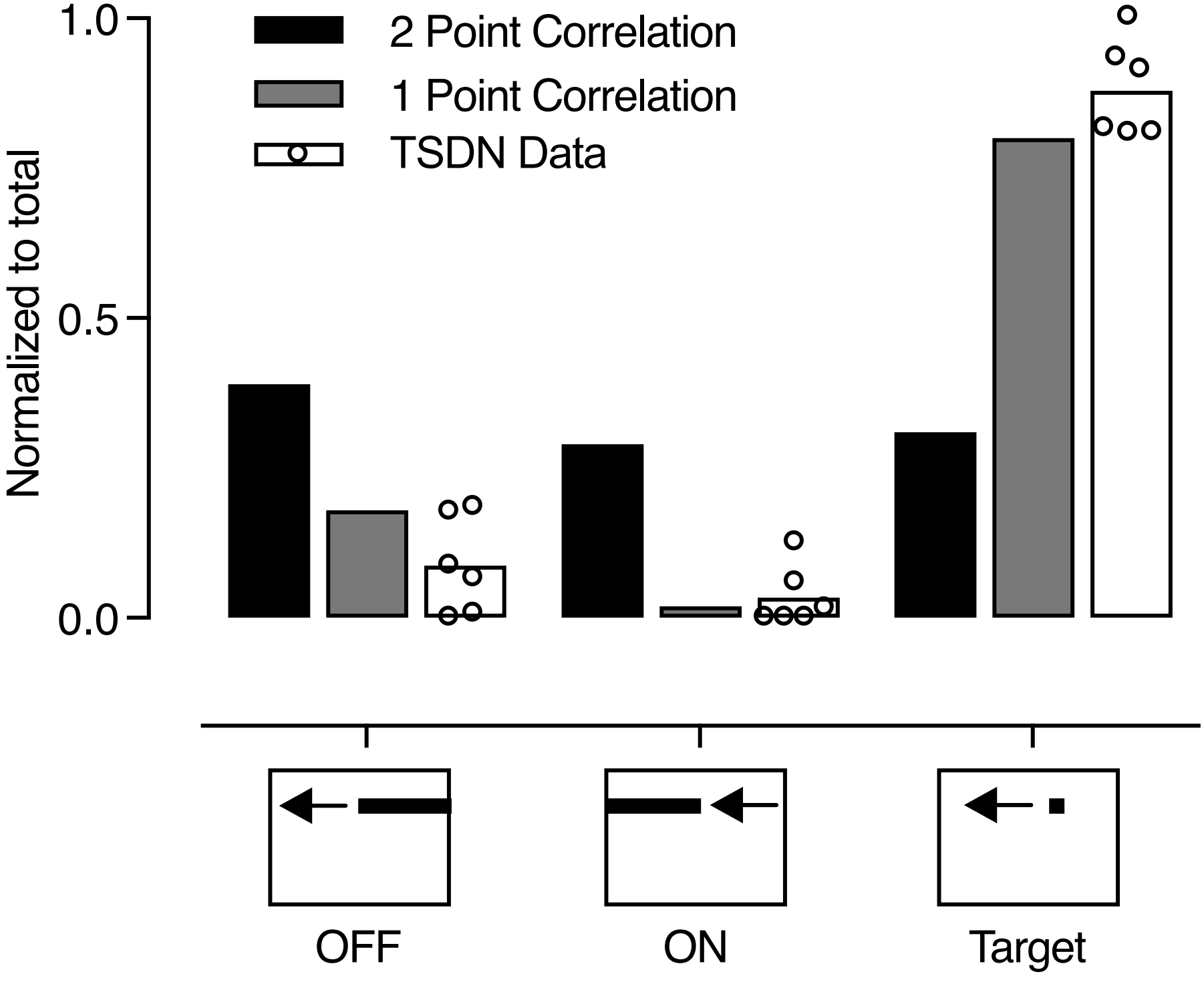
1.0
0.5
0.0
Normalized to total
2 Point Correlation
1 Point Correlation
TSDN Data
OFF
ON
Target

Figure 6